

RECURRENT GRAPH TENSOR NETWORKS

Yao Lei Xu, Danilo P. Mandic

Department of Electrical and Electronic Engineering, Imperial College London, SW7 2AZ, UK
 E-mails: {yao.xu15, d.mandic}@imperial.ac.uk

ABSTRACT

Recurrent Neural Networks (RNNs) are among the most successful machine learning models for sequence modelling. In this paper, we show that the modelling of hidden states in RNNs can be approximated through a multi-linear graph filter, which describes the directional flow of temporal information. The so derived multi-linear graph filter is then generalized to a tensor network form to improve its modelling power, resulting in a novel Recurrent Graph Tensor Network (RGTN). To validate the expressive power of the derived network, several variants of RGTN models were proposed and employed for the task of time-series forecasting, demonstrating superior properties in terms of convergence, performance, and complexity. By leveraging the multi-modal nature of tensor networks, RGTN models were shown to out-perform a standard RNN by 23% in terms of mean-squared-error while using up to 86% less parameters. Therefore, by combining the expressive power of tensor networks with a suitable graph filter, we show that the proposed RGTN models can out-perform a classical RNN at a drastically lower parameter complexity, especially in the multi-modal setting.

Index Terms— Tensor Networks, Tensor Decomposition, Graph Neural Networks, Graph Signal Processing, Recurrent Neural Networks.

1. INTRODUCTION

Tensors and graphs have found numerous applications in neural networks, by offering promising solutions for improving deep learning systems. In this context, tensor methods have been used to relax computational complexity of neural networks [1], as well as to alleviate their notorious “black-box” nature [2]. Graph based methods have generalized classical convolutional neural networks to irregular data domains, resulting in graph neural networks that have achieved state-of-the-art results in many applications [3]. Despite promising results, there is a void in literature regarding the combination of both techniques to solve deep learning challenges, especially in the area of sequence modelling. To address this issue, we set out to investigate Recurrent Neural Networks (RNNs) [4], the *de facto* deep learning tool for sequence modelling, from a tensor and graph theoretic perspective.

Tensors are multi-linear generalization of vectors and matrices to multi-way arrays, which allows for a richer representation of the data that is not limited to the classical “flat-view” matrix approaches [5]. Recent developments in tensor manipulation have led to Tensor Decomposition (TD) techniques that can represent high dimensional tensors through a contracting network of smaller core tensors. Such TD techniques can be used to compress the number of parameters needed to represent high-dimensional data, and have found many applications in deep learning. Notably, it has been shown that TD techniques, such as Tensor-Train Decomposition (TTD) [6], can be used to compress neural networks considerably while maintaining comparable performance [1].

The field of Graph Signal Processing (GSP) generalizes traditional signal processing concepts to irregular domains [7], which are naturally represented as graphs. Developments in GSP have led to series of spatial and spectral based techniques that generalise the notion of frequency and locality to irregular domains, allowing for the processing of signals that takes into account the underlying data domain [8]. Several concepts developed in GSP have found application in neural networks, where graph filters can be implemented across multiple layers to incorporate graph information [3].

However, despite the promising results achieved in both fields, the full potential arising from the combination of tensors and graphs is yet to be explored, especially in the area of sequence modelling. To this end, we set out to investigate RNNs using the theoretical framework underpinning tensor networks and graph signal processing. More specifically, we show that the modelling of RNN hidden states can be approximated through a multi-linear graph filtering operation, which can be used in conjunction with tensor networks to create a novel *Recurrent Graph Tensor Network* (RGTN). Our experimental results confirm the superiority of the proposed RGTN models, demonstrating desirable properties in terms of convergence, performance, and complexity.

The rest of the paper is organised as follows. Section 2 introduces the necessary theoretical background regarding tensors, graphs, and RNNs. Section 3 derives the proposed RGTN models. Section 4 analyses the experimental results achieved by the proposed models, demonstrating their effectiveness. Finally, section 5 summarises the virtues of the introduced framework.

2. THEORETICAL BACKGROUND

A short theoretical background is presented below, covering several topics in tensor networks, graph signal processing, and recurrent neural networks. We refer the readers to [5], [7], and [4] for an in-depth investigation of the subjects.

2.1. Tensors and Tensor Networks

$\mathbf{X} \in \mathbb{R}^{I_1 \times I_2 \times \dots \times I_N}$	N -th order tensor of size $I_1 \times I_2 \times \dots \times I_N$
$\mathbf{X} \in \mathbb{R}^{I_1 \times I_2}$	Matrix of size $I_1 \times I_2$
$\mathbf{x} \in \mathbb{R}^{I_1}$	Vector of size I_1
$x \in \mathbb{R}$	Scalar
$x_{i_1 i_2 \dots i_N} = \mathbf{X}(i_1, i_2, \dots, i_N)$	(i_1, i_2, \dots, i_N) entry of \mathbf{X}

Table 1. Tensor, matrix, vector, and scalar notation.

An order- N tensor, $\mathbf{X} \in \mathbb{R}^{I_1 \times I_2 \times \dots \times I_N}$, represents an N -way array with N modes, where the n^{th} mode is of size I_n , for $n = 1, 2, \dots, N$. Scalars, vectors, and matrices are special cases of tensors of order 0, 1, and 2 respectively, as detailed in Table 1. A tensor can be *reshaped* into a matrix through the *matricization* process, while the reverse process is referred to as *tensorization* [5]. A tensor can also be reshaped into a vector through the *vectorization* process, which is denoted with the operator $\text{vec}(\cdot)$. The tensor indices in this paper are grouped according to the Little-Endian convention [9].

An (m, n) -contraction, denoted by \times_n^m , between an N -th order tensor, $\mathbf{A} \in \mathbb{R}^{I_1 \times \dots \times I_n \times \dots \times I_N}$, and an M -th order tensor, $\mathbf{B} \in \mathbb{R}^{J_1 \times \dots \times J_m \times \dots \times J_M}$, with equal dimensions $I_n = J_m$, yields a tensor of order $(N + M - 2)$, $\mathbf{C} \in \mathbb{R}^{I_1 \times \dots \times I_{n-1} \times I_{n+1} \times \dots \times I_N \times J_1 \times \dots \times J_{m-1} \times J_{m+1} \times \dots \times J_M}$, with entries defined as in (1) [5]. For the special case of matrices, $\mathbf{A} \in \mathbb{R}^{I_1 \times I_2}$ and $\mathbf{B} \in \mathbb{R}^{J_1 \times J_2}$, the contraction $\mathbf{A} \times_2^1 \mathbf{B}$ denotes the standard matrix multiplication \mathbf{AB} .

$$c_{i_1 \dots i_{n-1} i_n + 1 \dots i_N j_1 \dots j_{m-1} j_m + 1 \dots j_M} = \sum_{i_n=1}^{I_n} a_{i_1 \dots i_{n-1} i_n i_{n+1} \dots i_N} b_{j_1 \dots j_{m-1} i_n j_m + 1 \dots j_M} \quad (1)$$

A (left) Kronecker product between two tensors, $\mathbf{A} \in \mathbb{R}^{I_1 \times \dots \times I_N}$ and $\mathbf{B} \in \mathbb{R}^{J_1 \times \dots \times J_N}$, denoted by \otimes , yields a tensor of the same order, $\mathbf{C} \in \mathbb{R}^{I_1 J_1 \times \dots \times I_N J_N}$, with entries $c_{\overline{i_1 j_1}, \dots, \overline{i_N j_N}} = a_{i_1 \dots i_N} b_{j_1 \dots j_N}$, where $\overline{i_n j_n} = j_n + (i_n - 1) J_n$ [5]. For the special case of matrices $\mathbf{A} \in \mathbb{R}^{I_1 \times I_2}$ and $\mathbf{B} \in \mathbb{R}^{J_1 \times J_2}$, the Kronecker product yields a block-matrix:

$$\mathbf{A} \otimes \mathbf{B} = \begin{bmatrix} a_{i_1 i_2} \mathbf{B} & \dots & a_{i_1 I_2} \mathbf{B} \\ \dots & \dots & \dots \\ a_{I_1 i_2} \mathbf{B} & \dots & a_{I_1 I_2} \mathbf{B} \end{bmatrix} \quad (2)$$

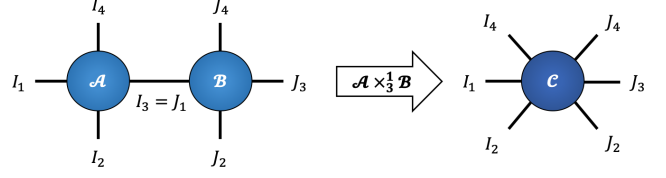


Fig. 1. Tensor network representation of a contraction $\mathbf{A} \times_3^1 \mathbf{B}$ between tensors $\mathbf{A} \in \mathbb{R}^{I_1 \times I_2 \times I_3 \times I_4}$ and $\mathbf{B} \in \mathbb{R}^{J_1 \times J_2 \times J_3 \times J_4}$, over the modes with equal dimensions $I_3 = J_1$.

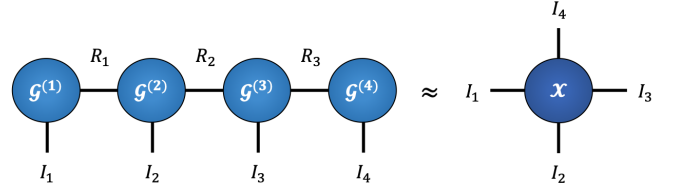


Fig. 2. Tensor network representation of TT decomposition for an order-4 tensor, $\mathbf{X} \in \mathbb{R}^{I_1 \times I_2 \times I_3 \times I_4}$, as in (3).

A tensor network admits a graphical representation of tensor contractions, where each tensor is represented as a node, while the number of edges that extend from that node corresponds to the tensor order [10]. If two nodes are connected through a particular edge, it represents a linear contraction over modes of equal dimensions represented by the edge. An example of tensor contraction in tensor network form is shown in Figure 1.

Special instances of tensor networks include Tensor Decomposition (TD) networks. The TD methods approximate high-order, large-dimensional tensors via contractions of smaller core tensors, which reduces the computational complexity drastically while preserving the data structure [10]. For instance, Tensor-Train decomposition (TTD) [11] [6] is a highly efficient TD method that can decompose a large order N tensor, $\mathbf{X} \in \mathbb{R}^{I_1 \times I_2 \times \dots \times I_N}$, into N smaller core tensors, $\mathbf{G}^{(n)} \in \mathbb{R}^{R_{n-1} \times I_n \times R_n}$, as:

$$\mathbf{X} = \mathbf{G}^{(1)} \times_2^1 \mathbf{G}^{(2)} \times_3^1 \mathbf{G}^{(3)} \times_3^1 \dots \times_3^1 \mathbf{G}^{(N)} \quad (3)$$

where the set of R_n for $n = 0, \dots, N$ and $R_0 = R_N = 1$ is referred to as the *TT-rank*. By virtue of TT, the number of entries in the original tensor is effectively reduced from $\prod_{n=1}^N I_n$ to $\sum_{n=1}^N R_{n-1} I_n R_n$, which is highly efficient for high N and low TT-rank. An example of TTD is shown in Figure 2.

2.2. Graph Signal Processing

A graph $\mathcal{G} = \{\mathcal{V}, \mathcal{E}\}$ is defined by a set of N vertices (or nodes) $v_n \in \mathcal{V}$ for $n = 1, \dots, N$, and a set of edges connecting the n^{th} and m^{th} vertices $e_{nm} = (v_n, v_m) \in \mathcal{E}$, for $n = 1, \dots, N$ and $m = 1, \dots, N$. A signal on a given graph is a defined by a vector $\mathbf{f} \in \mathbb{R}^N$ such that $\mathbf{f} : \mathcal{V} \rightarrow \mathbb{R}$, which associates a signal value to every node on the graph [12].

A given graph can be fully described in terms of its weighted adjacency matrix, $\mathbf{A} \in \mathbb{R}^{N \times N}$, such that $a_{nm} > 0$ if $e_{nm} \in \mathcal{E}$, and $a_{nm} = 0$ if $e_{nm} \notin \mathcal{E}$. Alternatively, the same graph can be described by its Laplacian matrix $\mathbf{L} \in \mathbb{R}^{N \times N}$ defined as $\mathbf{L} = \mathbf{D} - \mathbf{A}$, where $\mathbf{D} \in \mathbb{R}^{N \times N}$ is the diagonal degree matrix such that $d_{nn} = \sum_m a_{nm}$. In addition, both the weighted adjacency matrix and the Laplacian matrix can be presented in normalized form as $\tilde{\mathbf{A}} = \mathbf{D}^{-\frac{1}{2}} \mathbf{A} \mathbf{D}^{-\frac{1}{2}}$ and $\tilde{\mathbf{L}} = \mathbf{D}^{-\frac{1}{2}} \mathbf{L} \mathbf{D}^{-\frac{1}{2}}$ respectively [12].

In addition to capturing the underlying graph structure, both the Laplacian matrix and the weighted adjacency matrix can be used as shift operators to filter signals on graphs. Practically, a graph shift based filter results in a linear combination of vertex-shifted graph signals, which captures graph information at a local level [7]. For instance, the operation $\mathbf{g} = (\mathbf{I} + \mathbf{A})\mathbf{f}$ results in a filtered signal $\mathbf{g} \in \mathbb{R}^N$ such that:

$$g_n = f_n + \sum_{m \in \Omega_n} a_{nm} f_m \quad (4)$$

where Ω_n denotes the 1-hop neighbours that are directly connected to the n -th node. For M graph signals stacked in a matrix form as $\mathbf{F} \in \mathbb{R}^{N \times M}$, equation (4) can be compactly written as:

$$\mathbf{G} = (\mathbf{I} + \mathbf{A})\mathbf{F} \quad (5)$$

For reaching neighbours that are K -hops away, equation (4) can be extended to its polynomial form, as $\mathbf{g} = \sum_{k=0}^K h_k \mathbf{A}^k \mathbf{f}$, where h_k are constants [7]. Fundamentally, a K -hop based graph filter acts locally in the vertex space of a graph, which takes into account the irregular domain underlying the data described by its weighted adjacency matrix.

2.3. Recurrent Neural Networks

Recurrent Neural Networks (RNNs) [4] [13] are among the most successful deep learning tools for sequence modelling. A standard RNN layer captures time-varying dependencies by processing hidden states, $\mathbf{h}_t \in \mathbb{R}^M$, at time t through *feedback* or *recurrent* weights as:

$$\mathbf{h}_t = \sigma_h(\mathbf{W}^{(h)} \mathbf{h}_{t-1} + \mathbf{W}^{(x)} \mathbf{x}_t + \mathbf{b}^{(h)}) \quad (6)$$

where $\mathbf{h}_{t-1} \in \mathbb{R}^M$ is the hidden state vector from the previous time-step, $\mathbf{x}_t \in \mathbb{R}^N$ is the input features vector at time t , $\mathbf{W}^{(h)} \in \mathbb{R}^{M \times M}$ is the feedback matrix, $\mathbf{W}^{(x)} \in \mathbb{R}^{M \times N}$ is the input weight matrix, $\mathbf{b}^{(h)} \in \mathbb{R}^M$ is a bias vector, and $\sigma_h(\cdot)$ is an element-wise activation function.

Finally, after extracting the hidden states, these can be passed through additional weight matrices to generate outputs, $\mathbf{y}_t \in \mathbb{R}^P$ at time t , in the form:

$$\mathbf{y}_t = \sigma_y(\mathbf{W}^{(y)} \mathbf{h}_t + \mathbf{b}^{(y)}) \quad (7)$$

where $\mathbf{W}^{(y)} \in \mathbb{R}^{P \times M}$ is the output weight matrix, \mathbf{h}_t is the hidden state at time t , $\mathbf{b}^{(y)}$ is a bias vector, and $\sigma_y(\cdot)$ is an element-wise activation function.

3. RECURRENT GRAPH TENSOR NETWORKS

3.1. Special Recurrent Graph Filter

In this section, we derive the implicit graph filter underlying RNNs by considering a special case of the hidden state equation for modelling sequential data.

Consider a linear form of equation (6) without the bias term (non-linearity and bias can be introduced later on, as discussed in Section 3.3). Let $\hat{\mathbf{x}}_t = \mathbf{W}^{(x)} \mathbf{x}_t \in \mathbb{R}^M$ for $t = 1, \dots, \tau$ successive time-steps, then equation (6) can be written in block-matrix form as:

$$\begin{bmatrix} \mathbf{h}_\tau \\ \mathbf{h}_{\tau-1} \\ \vdots \\ \mathbf{h}_1 \end{bmatrix} = \begin{bmatrix} (\mathbf{W}^{(h)})^0 & (\mathbf{W}^{(h)})^1 & \cdots & (\mathbf{W}^{(h)})^{\tau-1} \\ 0 & (\mathbf{W}^{(h)})^0 & \cdots & (\mathbf{W}^{(h)})^{\tau-2} \\ \vdots & \vdots & \ddots & \vdots \\ 0 & 0 & \cdots & (\mathbf{W}^{(h)})^0 \end{bmatrix} \begin{bmatrix} \hat{\mathbf{x}}_\tau \\ \hat{\mathbf{x}}_{\tau-1} \\ \vdots \\ \hat{\mathbf{x}}_1 \end{bmatrix} \quad (8)$$

We now define: (i) $\hat{\mathbf{X}} \in \mathbb{R}^{\tau \times M}$ as the matrix generated by stacking, $\hat{\mathbf{x}}_t$, as row-vectors over τ successive time-steps; (ii) $\mathbf{H} \in \mathbb{R}^{\tau \times M}$ as the matrix generated by stacking hidden state vectors, \mathbf{h}_t , as row-vectors at corresponding time-steps; and (iii) $\mathbf{R} \in \mathbb{R}^{\tau M \times \tau M}$ as the block matrix composed by the powers of $\mathbf{W}^{(h)}$ from (8). This allows equation (8) to be expressed as:

$$\text{vec}(\mathbf{H}^T) = \mathbf{R} \times_2^1 \text{vec}(\hat{\mathbf{X}}^T) \quad (9)$$

Consider the special case of $\mathbf{W}^{(h)} = c\mathbf{I}^{(M)}$ where c is a positive constant less than 1, and $\mathbf{I}^{(M)} \in \mathbb{R}^{M \times M}$ is the identity matrix. This allows the hidden state equation to be expressed as $\mathbf{h}_t = c\mathbf{h}_{t-1} + \hat{\mathbf{x}}_t$, which represents a system where the past information is propagated to the future via a damping factor c . For this special case, we can simplify equation (8) as:

$$\mathbf{H} = \begin{bmatrix} 1 & c^1 & \cdots & c^{\tau-1} \\ 0 & 1 & \cdots & c^{\tau-2} \\ \vdots & \vdots & \ddots & \vdots \\ 0 & 0 & \cdots & 1 \end{bmatrix} \hat{\mathbf{X}} \quad (10)$$

Let $\mathbf{G} \in \mathbb{R}^{\tau \times \tau}$ denote the upper-triangular matrix in (10), then the same equation can be expressed in matrix form as $\mathbf{H} = \mathbf{G} \times_2^1 \hat{\mathbf{X}}$. Observe that matrix \mathbf{G} can be further decomposed as $\mathbf{G} = \mathbf{I}^{(\tau)} + \mathbf{A}$, where $\mathbf{I}^{(\tau)} \in \mathbb{R}^{\tau \times \tau}$ is the identity matrix and $\mathbf{A} \in \mathbb{R}^{\tau \times \tau}$ is the weighted adjacency matrix composed by the p -th powers of the constant c . Therefore, the special case of recurrent modelling can be expressed as:

$$\mathbf{H} = (\mathbf{I}^{(\tau)} + \mathbf{A}) \times_2^1 \hat{\mathbf{X}} \quad (11)$$

which is a form of localized graph filter as discussed in (5). For instance, each of the τ time-steps can now be considered as a node of a graph where signals are sampled from, and \mathbf{A} is the corresponding weighted graph adjacency matrix connecting different time-steps. This also justifies the triangular nature of the graph filter, since only past information can influence future states but not vice-versa.

3.2. General Recurrent Graph Filter

We now proceed to relax the restrictions from Section 3.1, to make it possible to extend the graph filter from (11) to the general case of sequence modelling.

Let the feedback matrix $\mathbf{W}^{(h)}$ be a scaled idempotent matrix, that is $\mathbf{W}^{(h)} = c\mathbf{W}^{(r)}$ where c is a positive constant less than 1 that models the damping effect, and $\mathbf{W}^{(r)}$ is an idempotent matrix that models how information propagates between successive time-steps. For this setup, the feedback matrix has the property $(\mathbf{W}^{(h)})^p = c^p\mathbf{W}^{(r)}$ for p greater than 0, which allows the block matrix \mathbf{R} to be simplified as:

$$\mathbf{R} = \begin{bmatrix} \mathbf{I}^{(M)} & c\mathbf{W}^{(r)} & \dots & c^{\tau-1}\mathbf{W}^{(r)} \\ 0 & \mathbf{I}^{(M)} & \dots & c^{\tau-2}\mathbf{W}^{(r)} \\ \vdots & \vdots & \ddots & \vdots \\ 0 & 0 & \dots & \mathbf{I}^{(M)} \end{bmatrix} \quad (12)$$

The block matrix \mathbf{R} with above properties can be further decomposed by using: (i) the weighted graph adjacency matrix, \mathbf{A} , from equation (11); (ii) the idempotent matrix, $\mathbf{W}^{(r)}$; and (iii) the identity matrix, $\mathbf{I}^{(\tau M)} \in \mathbb{R}^{\tau M \times \tau M}$, to yield:

$$\mathbf{R} = \mathbf{I}^{(\tau M)} + (\mathbf{A} \otimes \mathbf{W}^{(r)}) \quad (13)$$

which allows us to express equation 9 in its full form as:

$$\text{vec}(\mathbf{H}^T) = (\mathbf{I}^{(\tau M)} + (\mathbf{A} \otimes \mathbf{W}^{(r)})) \times_2^1 \text{vec}(\hat{\mathbf{X}}^T) \quad (14)$$

Finally, we define the multi-linear graph filter, $\mathcal{R} \in \mathbb{R}^{\tau \times M \times \tau \times M}$, to be the 4-th order tensorization of the block matrix, $\mathbf{R} \in \mathbb{R}^{\tau M \times \tau M}$, from equation (13). This allows us to simplify the expression in (14) without the vectorization operator by means of a double tensor contraction, as:

$$\mathbf{H} = \mathcal{R} \times_{3,4}^{1,2} \hat{\mathbf{X}} \quad (15)$$

This indicates that the graph structure discussed in Section 3.1 can be considered for the general case of sequence modelling, resulting in a multi-linear graph filter, \mathcal{R} , capable of modelling sequential information defined on a time-vertex graph domain.

3.3. Tensor Network Formulation

We next introduce a number of novel Recurrent Graph Tensor Network (RGTN) models, which benefit from the expressive power of tensor networks and the graph filters derived in the previous sections.

Consider the special case of graph filtering in section 3.1, where the hidden states are extracted through a graph filter that is localized in the vertex space. The extracted hidden states can be considered as feature maps, which can be flattened and passed through additional dense layers to generate application dependent outputs [14]. Using the tensor network notation, we can represent the special graph filter contraction and the dense layer matrix contraction as a unique tensor network, as shown in Figure 3. We refer to this special graph filter based tensor network as the special Recurrent Graph Tensor Network (*sRGTN*).

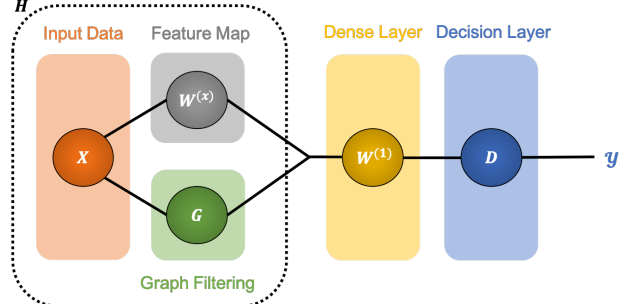


Fig. 3. Illustration of the *sRGTN* Model. The encircled section in dotted line represents the special graph filtering operation for extracting hidden states \mathbf{H} as introduced in (11).

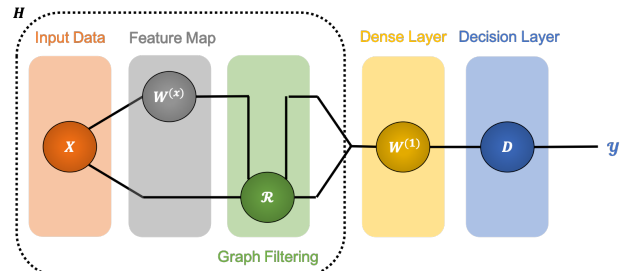


Fig. 4. Illustration of the *gRGTN* Model. The encircled section in dotted line represents the general graph filtering operation for extracting hidden states, \mathbf{H} , as introduced in (15).

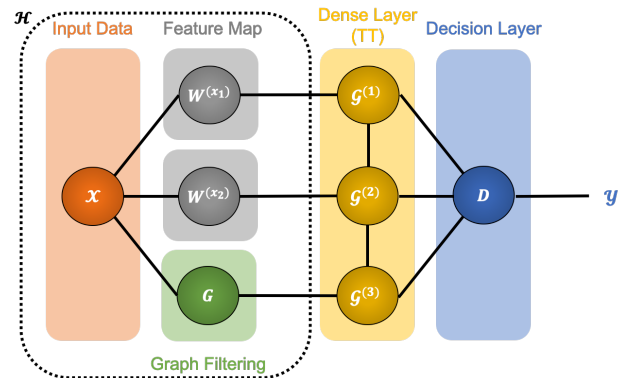


Fig. 5. Illustration of the *sRGTN-TT* Model. The encircled section in dotted line denotes the special graph filtering operation for extracting hidden states, \mathcal{H} , given a multi-modal input. The dense layer matrix (in yellow) is tensorized and represented in a tensor-train format to reduce complexity.

For the general case of graph filtering in Section 3.2, we can similarly represent the double contraction in (15) to derive the tensor network in Figure 4. This is referred to as the general Recurrent Graph Tensor Network (*gRGTN*). Unlike the *sRGTN* in Figure 3, where the graph filter and the feature map contractions can be modelled separately, *gRGTN* implies a stronger coupling of the features with the underlying graph domain, as captured by the multi-linear graph filter \mathcal{R} .

For multi-modal problems, we propose a highly efficient variant of the sRGTN by appealing to the super-compression power of the TTD. Indeed, by reshaping dense layer matrices into higher order tensors and representing them in a TT format, we can drastically reduce the parameter complexity, as discussed in [1]. This allows us to simultaneously: (i) maintain the inherent tensor structure of the problem; (ii) drastically reduce the parameter complexity of the model; and (iii) incorporate the underlying graph topology. This leads to the Multi-Modal, Tensor-Train variant of sRGTN (*sRGTN-TT*), which is illustrated in Figure 5.

Finally, non-linearity can be introduced into all considered models by applying a point-wise activation function on top of a contraction. Non-linear layers can also be stacked one after another to increase the overall expressive power.

4. EXPERIMENTS

4.1. Experimental Setting

In this section, the proposed Recurrent Graph Tensor Network (RGTN) models are implemented and compared to a standard Recurrent Neural Network (RNN) to validate the proposed models for the task of time-series forecasting.

The learning task of this experiment is to forecast the PM2.5 level across multiple sites in China, using the Beijing Multi-Site Air-Quality dataset [15]. Specifically, the data consists of hourly air quality measurements of 12 variables (PM2.5, PM10, SO2, NO2, CO, O3, TEMP, PRES, DEWP, RAIN, wd, WSPM) between 2013 and 2017 across 12 different geographical sites.

The given dataset is pre-processed by: (i) filling the missing data points with the corresponding feature median; (ii) scaling the numerical features between 0 and 1; and (iii) encoding the categorical features via one-hot-encoding, which increases the number of total features to 27 per site.

For the given task, a total of 4 models were implemented and compared. To achieve comparable results, all models were given the same architectural specification, as shown in Table 2, with the only difference being the choice of feature extraction method. Specifically, the four feature extraction methods are based on: (i) a simple recurrent neural network (RNN); (ii) a special Recurrent Graph Tensor Network (sRGTN), which implements the architecture in Figure 3; (iii) a general Recurrent Graph Tensor Network (gRGTN), which implements the architecture in Figure 4; and (iv) a sRGTN with TT decomposition (sRGTN-TT), which implements the architecture in Figure 5. Finally, all the models were trained with the same setting, that is using: (i) a stochastic gradient descent optimizer with a learning rate of 10^{-4} ; (ii) a mean-squared-error loss function; (iii) a batch size of 32; and (iv) a total of 100 epochs. The first 70% of the data was used for training purposes (20% of which is used for validation), and the remaining 30% for testing.

RNN Model	Layer 1	Layer 2	Layer 3
Layer Type	<i>RNN</i>	<i>Dense</i>	<i>Dense</i>
Units	8	12	12
Activation	<i>tanh</i>	<i>tanh</i>	<i>linear</i>

sRGTN Model	Layer 1	Layer 2	Layer 3
Layer Type	<i>sRGTN</i>	<i>Dense</i>	<i>Dense</i>
Units	8	12	12
Activation	<i>tanh</i>	<i>tanh</i>	<i>linear</i>

gRGTN Model	Layer 1	Layer 2	Layer 3
Layer Type	<i>gRGTN</i>	<i>Dense</i>	<i>Dense</i>
Units	8	12	12
Activation	<i>tanh</i>	<i>tanh</i>	<i>linear</i>

sRGTN-TT Model	Layer 1	Layer 2	Layer 3
Layer Type	<i>sRGTN</i>	<i>TT-Dense</i>	<i>Dense</i>
Units	8	12	12
Activation	<i>tanh</i>	<i>tanh</i>	<i>linear</i>
TT-Rank	<i>n.a.</i>	<i>(1,2,2,1)</i>	<i>n.a.</i>

Table 2. Architecture of the models used in the experiment.

Note that for the sRGTN-TT model, each input data sample, $\mathcal{X} \in \mathbb{R}^{6 \times 12 \times 27}$, was kept in its natural multi-modal form, which contains 6 consecutive time-steps of data across 12 different sites, where each site contains 27 features. For the RNN, sRGTN, and gRGTN models, each of the input data sample, $\mathbf{X} \in \mathbb{R}^{6 \times 324}$, was a matrix created by concatenating 27 features per site across all 12 sites (324 features in total) over 6 consecutive time-steps. For all models, the target prediction variable, $\mathbf{y} \in \mathbb{R}^{12}$, is the PM2.5 measurement of the successive time-step across all 12 sites.

4.2. Experiment Results

	RNN	sRGTN	gRGTN	sRGTN-TT
N. Param.	3408	3384	3448	463
Test MSE	0.010935	0.009998	0.009183	0.008467

Table 3. The number of trainable parameters and the Test MSE for all proposed models. The sRGTN-TT obtained the best results with a drastically lower number of parameters.

This section analyses the results obtained from the proposed experiment, demonstrating the superior properties of the proposed RGTN models over a standard RNN model, in terms of convergence, performance, and complexity properties, especially in the multi-modal setting.

Table 4.2 shows the number of trainable parameters and the final test Mean-Squared-Error (MSE) achieved by the four considered models. Simulation results confirm the superiority of the proposed class of RGTN models over a standard RNN, especially in the multi-modal setting. In particular, the proposed *sRGTN-TT* model successfully captured the inherent multi-modality of the underlying problem, achieving the best MSE score while using up to 86% less parameters than other models.

Figure 6 shows the validation MSE of all four considered models during the training phase (in log scale). The error curves show that all RGTN models exhibited better convergence properties than the standard RNN model, as fewer epochs were needed to converge.

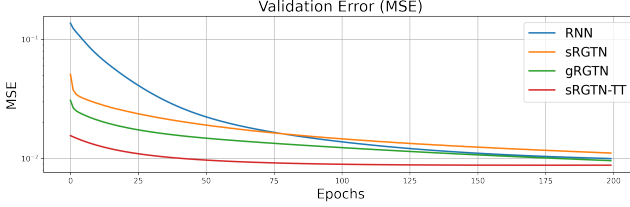


Fig. 6. Validation MSE over 100 epochs of training, for all considered models. The RGTN models exhibited faster convergence and enhanced performance over the RNN.

5. CONCLUSION

We have proposed a novel Recurrent Graph Tensor Network (RGTN) architecture, by merging the expressive power of tensor networks with graph signal processing methods over irregular domains. We have provided the theoretical framework underpinning the proposed RGTN models and applied them to the task of time-series forecasting. The experimental results have shown that the proposed class of RGTN models exhibits desirable properties in terms of convergence, performance, and complexity. In particular, when dealing with multi-modal data, the proposed RGTN models have out-performed a standard RNN both in terms of performance (23% improvement in mean-squared-error) and complexity (86% reduction in trainable parameters).

6. REFERENCES

- [1] A. Novikov, D. Podoprikin, A. Osokin, and D. P. Vetrov, “Tensorizing neural networks,” in *Proceedings of the Advances in Neural Information Processing Systems (NIPS)*, 2015, pp. 442–450.
- [2] N. Cohen, O. Sharir, and A. Shashua, “On the expressive power of deep learning: A tensor analysis,” in *Proceedings of Conference on Learning Theory*, 2016, pp. 698–728.
- [3] Z. Wu, S. Pan, F. Chen, G. Long, C. Zhang, and S. Y. Philip, “A comprehensive survey on graph neural networks,” *IEEE Transactions on Neural Networks and Learning Systems*, 2020.
- [4] D. P. Mandic and J. Chambers, *Recurrent neural networks for prediction: Learning algorithms, architectures and stability*, John Wiley & Sons, Inc., 2001.
- [5] A. Cichocki, “Era of big data processing: A new approach via tensor networks and tensor decompositions,” *ArXiv e-prints*, Mar. 2014.
- [6] I. V. Oseledets, “Tensor-train decomposition,” *SIAM Journal on Scientific Computing*, vol. 33, no. 5, pp. 2295–2317, 2011.
- [7] L. Stankovic, D. Mandic, M. Dakovic, M. Brajovic, B. Scalzo, and A. G. Constantinides, “Graph signal processing—Part II: Processing and analyzing signals on graphs,” *arXiv preprint arXiv:1909.10325*, 2019.
- [8] M. M. Bronstein, J. Bruna, Y. LeCun, A. Szlam, and P. Vandergheynst, “Geometric deep learning: Going beyond Euclidean data,” *IEEE Signal Processing Magazine*, vol. 34, no. 4, pp. 18–42, 2017.
- [9] S.V. Dolgov and D.V. Savostyanov, “Alternating minimal energy methods for linear systems in higher dimensions,” *SIAM Journal on Scientific Computing*, vol. 36, no. 5, pp. A2248–A2271, 2014.
- [10] A. Cichocki, N. Lee, I. Oseledets, A. Phan, Q. Zhao, D. P. Mandic, et al., “Tensor networks for dimensionality reduction and large-scale optimization: Part 1 Low-rank tensor decompositions,” *Foundations and Trends® in Machine Learning*, vol. 9, no. 4-5, pp. 249–429, 2016.
- [11] I. V. Oseledets and E. E. Tyrtyshnikov, “Breaking the curse of dimensionality, or how to use SVD in many dimensions,” *SIAM Journal on Scientific Computing*, vol. 31, no. 5, pp. 3744–3759, 2009.
- [12] L. Stankovic, D. P. Mandic, M. Dakovic, M. Brajovic, B. Scalzo, and T. Constantinides, “Graph signal processing—Part I: Graphs, graph spectra, and spectral clustering,” *arXiv preprint arXiv:1907.03467*, 2019.
- [13] Y. Khalifa, D. P. Mandic, and E. Sejdic, “The role of hidden markov models and recurrent neural networks in event detection and localization for biomedical signals: Theory and application,” *Information Fusion*, 2020.
- [14] M. Z. Alom, T. M. Taha, C. Yakopcic, S. Westberg, P. Sidike, M. S. Nasrin, M. Hasan, B. C. Van Essen, A. Awwal, and V. K. Asari, “A state-of-the-art survey on deep learning theory and architectures,” *Electronics*, vol. 8, no. 3, pp. 292, 2019.
- [15] S. Zhang, B. Guo, A. Dong, J. He, Z. Xu, and S. X. Chen, “Cautionary tales on air-quality improvement in beijing,” *Proceedings of the Royal Society A: Mathematical, Physical and Engineering Sciences*, vol. 473, no. 2205, pp. 20170457, 2017.